## RESEARCH

# Extensive immunophenotypic sub-population analysis of StemRegenin1 expanded haematopoietic stem/progenitor cells

Juanita Mellet[1†], Candice L. Hendricks[1†], Voula Stivaktas[2], Chrisna Durandt[1], Melvin A. Ambele[1,3] and Michael S. Pepper[1*]

## Abstract

**Background** Ex vivo haematopoietic stem/progenitor cell (HSPCs) expansion constitutes an important area of research, and has the potential to improve access to umbilical cord blood (UCB) as a source of stem cells for haematopoietic stem cell transplantation (HSCT). The ability to improve stem cell dose and thereby reduce delayed engraftment times, which has plagued the use of UCB as a stem cell source since inception, is a recognised advantage. The extent to which cluster of differentiation (CD)34 sub-populations are affected by expansion with StemRegenin1 (SR1), and whether a particular subtype may account for better engraftment than others, is currently unknown. The purpose of this study was to determine the impact of SR1-induced HSPC expansion on CD34+ immunophenotypic subsets and gene expression profiles.

**Methods** UCB-derived CD34+ HSPCs were characterised before (D0) and after expansion (D7) with SR1 using an extensive immunophenotypic panel. In addition, gene expression was assessed and differentially expressed genes were categorised into biological processes.

**Results** A dose-dependent increase in the number of CD34+ HSPCs was observed with SR1 treatment, and unbiased and extensive HSPC immunophenotyping proved to be a powerful tool in identifying unique sub-populations within the HSPC repertoire. In this regard, we found that SR1 promotes the emergence of HSPC subsets which may aid engraftment post expansion. In addition, we observed that SR1 has a minimal effect on the transcriptome of 7-day expanded CD34+ HSPCs when compared to cells expanded without SR1, with only two genes being downregulated in the former.

**Conclusion** This study revealed that SR1 selects for potentially novel immunophenotypic HSPC subsets post expansion and has a minimal effect on the transcriptome of 7-day expanded HSPCs when compared to vehicle controls. Whether these distinct immunophenotypic sub-populations possess greater engraftment capacity remains to be tested in animal models.

---

[†]Juanita Mellet and Candice L. Hendricks contributed equally as first authors.

*Correspondence:
Michael S. Pepper
michael.pepper@up.ac.za

Full list of author information is available at the end of the article

## Background

The first paediatric umbilical cord blood (UCB) transplantation (UCBT) in a child with Fanconi anaemia in 1988 [1] opened an exciting and pivotal area of research and treatment. Subsequently however, the limited number of cluster of differentiation (CD)34+ haematopoietic stem and progenitor cells (HSPCs) in a single UCB unit has meant that in order to reach the optimal CD34+ cell dose for haematopoietic stem cell transplantation (HSCT) of $1\text{-}1.75\times10^5$ cells/kg body weight [2], two or more UCB units need to be combined for UCBT in adults. This is done to overcome the consequence of delayed engraftment [3] and the ensuing increased risk of infection, hospitalisation and non-relapse mortality [4]. With present global trends showing a decline in UCB use as an HSPC source [5] due to these disadvantages, ex vivo expansion of HSPCs has provided a potential opportunity to put UCBT "back on the map".

Expansion of HSPCs outside their natural environment is challenging, since in vitro culture conditions induce spontaneous differentiation resulting in reduced stem cell characteristics. Numerous efforts have been made to expand these cells and to simulate their natural environment in vitro. These efforts have been aimed at identifying ex vivo conditions that promote self-renewal and proliferation of HSPCs, while at the same time restricting their differentiation. The cytokine combination consisting of stem cell factor (SCF), FMS-like tyrosine kinase 3 ligand (FLT3L), and thrombopoietin (TPO) has been extensively studied for the ex vivo expansion of HSPCs, collectively referred to as "early acting" cytokines [6]. These cytokines are used in several clinical and preclinical HSPC expansion protocols [7–9] and have been shown to promote quiescence and self-renewal [10]. The use of interleukin (IL)-3 and IL-6 is critical for the expansion of CD133+ HSPCs, with IL-6 being important in maintaining an immature HSPC phenotype following expansion [11]. Expansion of HSPCs exclusively with cytokines has not significantly improved engraftment parameters [12], and thus harnessing intrinsic regulators and biochemical pathways through the use of small molecules has been employed to support expansion. Supplementing ex vivo HSPC cultures with nicotinamide (NAM), a form of vitamin B3, resulted in delayed differentiation and increased engraftment of UCB-derived CD34+ HSPCs. Expansion in the presence of NAM increases the number of early HSPCs (CD34+CD38−) and decreases the number of lineage-restricted cells [13]. StemRegenin1 (SR1), an aryl hydrocarbon receptor (AhR) antagonist, has also been used for the ex vivo expansion of CD34+ HSPCs with long-term engraftment potential [14–16]. SR1 was discovered during an unbiased screening of a library of potential compounds using primary human HSPCs [15]. Recent studies have further explored the impact of SR1 on haematopoietic lineages [16–18]. Furthermore, it has shown to maintain the expression of stem cell markers, including CD34 on endothelial progenitor cells [19]. AhR regulates the effect of environmental toxins and plays a role in modulating haematopoiesis and the immune system [16] through its role as a DNA-binding transcription factor [20]. A phase I/II clinical trial has demonstrated improved neutrophil and platelet engraftment following UCBT with a single ex vivo SR1-expanded UCB unit [9].

The assessment of expanded UCB HSPCs as a standalone treatment is underway in clinical trials [21, 22]. This approach could be an important option in South Africa, where the cost of procuring two stand-alone UCB units is prohibitive and the identification of potential HSCT donors is difficult. Indeed, the odds of finding a match for HSCT are about 75% for individuals of European descent [23], while this drops to <20% for ethnolinguistic groups of sub-Saharan African descent [23]. We could thus capitalise on the major advantage of UCB, which is a less stringent human leukocyte antigen (HLA)-matching requirement when compared to other stem cell sources [24], particularly in a setting such as our own in which the genetic diversity in sub-Saharan African populations may be restrictive [25].

Expanded UCB plays an important role in the context of limited donor availability, and it has the potential to make a local public UCB bank more cost-effective by utilising UCB units that are historically inadequate in terms of cell numbers [26]. Furthermore, should a particular immunophenotypic subset of CD34+ HSPCs be found to harbour superior intrinsic engraftment capacity after expansion, an expansion agent may be found to be superior to others. An example may be revealing stem cell subsets with known 'true' stem cell markers such as CD90 and CD49f [27], which can be exploited for the purposes of HSCT. Some studies have shown that the Lin-CD34+CD38-CD133+CD45RA- population harbours multipotent progenitors (MPP) [28, 29] while others believe true stem cells exist in the CD34+CD90+ population, with an approximate frequency of 0.2% in the CD34+ population [30]. The identification of specific immunophenotypic subsets within CD34+ HSPCs may thus provide insight into how expansion affects these cells. Limited immunophenotypic data is available in the literature on the impact of expansion with SR1 on CD34+ HSPC

subsets [9, 15, 18, 31]. Additionally, there is limited data on the effect of SR1 on the side population (SP), an indication of stem cell primitivity [32] as well as on the gene expression profiles of expanded CD34+ cells [15, 31] and how this compares to gene expression in non-expanded CD34+ cells.

The purpose of this study was to provide detailed analyses on the impact of SR1 on CD34+ HSPCs from UCB by means of extensive unsupervised clustering immunophenotyping analysis, SP analysis after in vitro expansion and gene expression analysis of CD34+ HSPCs before and after expansion.

## Materials and methods
### Sample collection
Informed consent was obtained from healthy human immunodeficiency virus (HIV)-negative mothers scheduled for caesarean section at 37 to 40 weeks gestation at a private hospital in Pretoria, South Africa. UCB was collected into bags containing citrate phosphate dextrose anticoagulant (Tianhe Pharmaceutical, China), stored at 4°C and used within 24 h. The HIV status of the mothers was obtained from their files or verbally during informed consent, and confirmed using the GeneXpert 1 System (Cepheid, USA) and Xpert® HIV-1 Qual or HIV-1 Qual XC cartridges (Cepheid, USA). Three individual donor samples were used for SR1 concentration optimisation, three samples for the 4-colour immunophenotype panel, and five samples for the 8-colour immunophenotype panel. For the gene expression, three pooled samples (each containing two UCB units) were used.

### CD34+ HSPC enrichment
UCB was layered onto Histopaque®-1077 (Sigma-Aldrich, USA) in sterile 50 mL Falcon tubes at a 2:1 volume ratio and centrifuged for 30 min at 388 x *g*. The plasma fraction was aspirated, and the mononuclear cell (MNC) layer collected. Red blood cells were lysed using ammonium chloride ($NH_4Cl$, pH 7.4) and the samples incubated at 4°C. Samples were centrifuged at 300 x *g* for 10 min at 4°C and $NH_4Cl$ was aspirated after which the cells were washed twice with TP buffer [phosphate buffered saline (PBS, pH 7.4), 10 µg/mL human albumin (Sigma-Aldrich, USA), and 2 mM ethylenediaminetetraacetic acid (EDTA)]. The supernatant was aspirated, and the cells were resuspended in up to 10 mL of TP buffer. A MNC aliquot was stained with CD45 (clone J33) FITC, CD34 (clone 581) PE and the viability dye, 7AAD (Stem-Kit™ HSPC enumeration kit, Beckman Coulter, Miami, USA) to identify viable CD34+ HSPCs. A second aliquot of the MNC suspension was stained with CD45 FITC (clone J33) and IsoClonic control PE and 7AAD (Stem-Kit™ HSPC enumeration kit, Beckman Coulter, Miami, USA) to determine the negative/positive boundary of CD34

expression. Viable CD34+ cells from the MNC fraction were sorted into 24-well plates using the BD FACSAria™ Fusion cell sorter (BD Biosciences, USA). Sorting purities of >90% were achieved. Depending on the experiment, CD34+ HSPCs were sorted into serum-free expansion medium (StemSpan ACF/AOF; StemCell Technologies, Canada) or directly into lysis buffer (Qiagen, Germany).

### Culture conditions
CD34+ HSPCs were cultured in 24-well plates ($1 \times 10^4$ cells/well) in 1 mL StemSpan ACF/AOF medium supplemented with 2% penicillin (100 units/mL, GibcoBRL, USA), streptomycin (0.1 mg/mL, GibcoBRL, USA) and recombinant human growth factors, each at 100 ng/mL: SCF, TPO, FLT3L, granulocyte colony-stimulating factor (G-CSF) and IL-3 (Life Technologies, Thermo Fisher Scientific, USA). Cytokine combinations were optimised prior to starting these experiments (Additional file 1: Tables S1-2 and Figures S1-S6). Cultures were maintained at 37°C and 5% $CO_2$ in a humidified atmosphere for 7–8 days. SR1 (StemCell Technologies, Canada) was dissolved in dimethyl sulfoxide (DMSO; Sigma-Aldrich, USA) and further dilutions were made using StemSpan ACF/AOF. The following concentrations were tested to determine the optimal SR1 concentration for HSPC expansion: 0.25, 0.5, 0.75 and 1 µM. A vehicle control (VC) containing DMSO (0.01%) was included. Subsequent expansion, immunophenotype and gene expression experiments were performed using 1 µM SR1.

### Flow cytometry
Two separate antibody panels, one with four and another with eight colours, were used to determine viability and CD34+ percentages on Day 0 (D0) and Day 7 (D7). The 4-colour immunophenotype panel was acquired using a 3-laser, 10-colour Gallios flow cytometer (Beckman Coulter, Miami, USA), while the subsequent larger 8-colour panel was acquired using a CytoFLEX flow cytometer (Beckman Coulter, Miami, USA). The D7 subsets were analysed in those cells expanded with (SR1) and without SR1 (VC).

The 4-colour immunophenotypic panel included the following anti-human monoclonal antibodies: Lin FITC (clones: CD3, UCHT1; CD14, HCD14; CD16, 3G8; CD19, HIB19; CD20, 2H7; CD56, HCD56; BioLegend, USA), CD34 PE-Cy7 (clone: 581; BioLegend, USA), CD38 APC-Cy7 (clone: HIT2; BioLegend, USA), CD133/2 PE (clone: 293C3; Myltenyi Biotec, Germany) and Mouse IgG2b PE isotype (clone: IS6-11E5.11; Myltenyi Biotec, Germany). The analysis was performed using either a Gallios flow cytometer or BD FACSAria Fusion cell sorter. Post-acquisition analyses were performed using Kaluza Analysis Software (version 2.1; Beckman Coulter, Miami, USA). The flow cytometric protocol and gating

strategy are summarised in Additional file 2: Fig. S1. Fold increase in absolute cell numbers as well as percentage was used to determine cell sub-populations before and after a 7-day expansion. Fold increase refers to the factor by which the number of cells observed on D7 increased relative to the number of cells seeded on D0, and was calculated as follows:

$$Fold\ Increase = \frac{Total\ number\ of\ cells\ on\ D7 - Total\ number\ of\ cells\ seeded\ on\ D0}{Total\ number\ of\ cells\ seeded\ on\ D0}$$

The 8-colour immunophenotype panel included the following anti-human monoclonal antibodies: Lin FITC (clones: CD3, UCHT1; CD14, HCD14; CD16, 3G8; CD19, HIB19; CD20, 2H7; CD56, HCD56; BioLegend, USA), CD34 APC AF700 (clone: 581; Beckman Coulter, Miami, USA), CD38 ECD (clone: LS198-4-3; Beckman Coulter, Miami, USA), CD133 PE-Violet 770 (clone: REA753; Miltenyi Biotec, Germany), CD117 PE (clone: 104D2; BioLegend, USA), CD90 BV510 (clone: 5E10; BioLegend, USA), CD45RA APC (clone: 2H4; Beckman Coulter, Miami, USA), CD49f SB780 (clone: G0H3; BioLegend, USA). Prior to determining the antibody volumes for the 8-colour panel, antibody titrations were performed and decisions on volumes were made based on the staining index [Stain Index = (Median of Positive − Median of Negative) / (Standard Deviation of Negative * 2)]. Post-acquisition analyses were performed using Kaluza Analysis Software (version 2.1; Beckman Coulter, Miami, USA) and Cytobank software (http://www.cytobank.org; Beckman Coulter, Miami, USA). The gating strategy employed prior to Cytobank analysis is summarised in Additional file 2: Fig. S2. Once uploaded into the Cytobank platform, data clean-up was performed using Peak Extraction and Cleaning Oriented Quality Control (PeacoQC) to identify and exclude any anomalous events. For the description of the D0 and D7 immunophenotype, all associated files were concatenated prior to Cytobank analysis. For statistical analysis, sample files were analysed individually and compared. Dimensionality reduction was performed using t-distributed stochastic neighbour embedding (tSNE) plots, after which a flow cytometry self-organising map (FlowSOM) was performed to determine statistically significant differences in populations in the D7 subsets (SR1 versus VC) using box plots and heat maps. Statistical analysis was performed using non-parametric Kruskal-Wallis and Mann-Whitney U tests where appropriate.

## Side population (SP) analysis

SP analysis has proven to be a valuable tool to identify a population of immature HSPCs [33]. SP data was obtained from two different donors. Primitive (immature) stem cells preferentially efflux cytoplasmic lipophilic fluorescent dyes, such as the DNA binding dyes Vybrant® DyeCycle™ (VDC) Violet and Hoechst, resulting in a sub-population of cells displaying lower fluorescent intensity levels. The SP fraction (displayed as a percentage) was identified as cells with higher dye efflux ability and therefore cells with low/negative VDC Violet fluorescence compared to the rest of the population. SP analysis was performed after eight days in culture. Triplicate wells were pooled for SP analysis at a concentration of $10^3$ viable cells/μL medium, in a total of 1 mL per tube. A Verapamil control (100 μM; Sigma-Aldrich, USA) was included for each condition. VDC Violet (5 μg/mL; Life Technologies, Thermo Fisher Scientific, USA) was added to all tubes and incubated at 37°C for 120 min, protected from light. Following incubation, cells were placed on ice and analysed on the BD FACSAria Fusion. Cells were stained with Annexin V FITC (Beckman Coulter, Miami, USA), 7AAD, CD34 PE-Cy7 and CD38 APC-Cy7 prior to analysis. The flow cytometric protocol and gating strategy are summarised in Additional file 1: Fig. S3.

## RNA extractions, integrity and quality

The Qiagen RNeasy Micro Plus kit (Qiagen, Germany) was used to perform RNA extractions according to the manufacturer's instructions. Cells ($10^5$) were sorted into 300 μL lysis buffer and were kept at 4°C throughout the sorting process. RNA was extracted from two aliquots of cells ($10^5$ each) on D0 and concentrated by vacuum centrifugation using a SpeedVac SVC-100 (Savant Instruments, USA). RNA integrity and quality were assessed using the TapeStation® 2200 (Agilent Technologies, USA), RNA ScreenTape® (Agilent Technologies, USA) and Sample Buffer Kit (Agilent Technologies, USA).

## Gene expression

Gene expression analysis (50 ng total RNA in each sample) was performed using Affymetrix GeneChip® Human Gene 2.0 ST arrays (Affymetrix, USA) and Affymetrix GeneChip® WT PLUS Reagent Kit (Affymetrix, USA) according to the manufacturer's manual. Purified, fragmented and labelled complementary RNA was added to the hybridization cocktail using Hybridization Wash and Stain Kit (Affymetrix, USA). The hybridization cocktail was hybridized to Affymetrix GeneChip® Human Gene 2.0 ST arrays for 17 h. The GeneChips were placed in an Affymetrix GeneChip® Hybridization Oven-645 (Affymetrix, USA) at 45°C rotating at 60 rpm. The hybridized chips were washed and stained in an Affymetrix GeneChip® Fluidics Station-450Dx (Affymetrix, USA) before scanning using an Affymetrix GeneChip® Scanner-7G (Affymetrix). Analyses were performed using the Affymetrix Transcriptome Analysis Console™ (TAC) Software 4.0 (Affymetrix, USA). Genes with a fold change$\geq 2.5$ and $\leq -2.5$ and ($P < 0.05$) were

considered to be differentially expressed. The microarray data files of this study have been submitted to NCBI GEO (Gene Expression Omnibus) with accession number GSE146810. The Database for Annotation, Visualization, and Integrated Discovery (DAVID) analysis tool (https://david.ncifcrf.gov) was used to classify differentially expressed genes into biological processes [34].

### Statistical analysis

Experiments were performed in triplicate using two to eight independent UCB samples. Values represent mean±standard deviation (SD). Statistical analyses were performed using GraphPad Prism (Version 10.0.2) as well as the Cytobank platform. A non-parametric one- or two-way analysis of variance (ANOVA), a Kruskal-Wallis, a Mann-Whitney U test and a Dunn's Multiple Comparison Test were performed where appropriate to determine statistical significance ($P < 0.05$).

## Results

### SR1 concentration optimisation

#### *Expanded CD34+ sub-populations*

Mean Lin-CD34+HSPC percentages significantly increased ($p = 0.0349$) with increasing SR1 concentrations (Fig. 1a and b), recorded as 38.6±1.8% at 1 μM SR1, compared to 16.2±5.5% in the VC ($n = 3$). The Lin-CD34+CD38- population remained stable across the different SR1 concentrations ($p = 0.9453$), maintaining percentages of 66.4±2.8% at 1 μM SR1, in comparison to 63.3±4.3% in the VC (Fig. 1c). Meanwhile, the Lin-CD34+CD38-CD133+ sub-population showed a decrease in mean percentages with higher SR1 concentrations ($p = 0.0306$), recording 74.3±5.8% at 1μM SR1, as opposed to 87.9±5.3% in the VC (Fig. 1d). These experiments were performed on three biological replicates.

#### *Immunophenotyping of the side population sub-populations*

Side population (SP) experiments were performed on two biological replicates ($n = 2$). The SP disappeared when cells were treated with Verapamil (Fig. 1d), a calcium channel blocker. The SP had previously been identified in CD34+ [35, 36] and CD34- HSPCs [33, 36, 37] and was therefore investigated in our study in both CD34+CD38- and CD34-CD38- HSPCs. The mean percentage SP in the control was similar for CD34+CD38- (1.03±0.11%) and CD34-CD38- (1.04±0.20%) cells (Fig. 1e). Although not statistically significant when compared to the control, the highest mean percentage of SP cells was identified for both CD34+CD38- cells (1.40±1.34%) and CD34-CD38- cells (1.91±0.95%) using SR1 at 0.25 μM. In addition, and although not statistically significant, SP percentages were numerically higher in CD34-CD38- cells compared to CD34+CD38- cells for all SR1 concentrations (Additional file 1: Table S3). Additional file 1: Table S3 shows the percentage SP in CD34+CD38- and CD34-CD38- populations after expansion with SR1.

### Immunophenotyping

#### *Immunophenotyping using a 4-colour immunophenotype panel*

Immunophenotypic profiles using a 4-colour immunophenotypic panel were then assessed before and after expansion in the presence of SR1 at a concentration of 1 μM. Clear differences were observed between D0 and D7 immunophenotypic profiles of Lin-CD34+HSPCs. On D0, 54.7±7.9% of the Lin-CD34+population expressed CD133. The CD38 expression was continuous, making it difficult to set a boundary with manual gating (Additional file 2: Fig. S1).

On D7, a very small proportion of the cells were lineage positive. The most noticeable difference was the total proportion of Lin-CD34+HSPCs present on D7 after SR1 expansion (38.0±8.9%), which was larger than for control cells (22.9±11.9%), albeit not statistically significant (Fig. 2a). Within the Lin-CD34+population, 39.6±7.1% of cells were CD133-positive after SR1 expansion, which was lower than for control cells at 59.2±11.5% (Fig. 2a). Although the CD38-positive population within the Lin-CD34+population was still continuously expressed, it was easier to identify a CD38+ and CD38- population.

An additional five independent samples (total samples $n = 8$) were then expanded using SR1 at 1 μM to corroborate the data obtained from the three initial samples. Figure 2b shows the mean fold change in total viable cells for SR1 (89.2±29.4) compared to the VC (124.3±41.7). The total viable CD34+cell number was, however, increased by 42.8±15.4 versus 23.7±5.4, respectively. These changes confirm the potency of SR1 to increase CD34+cells, even though not statistically significant when compared to the VC. The contribution of each individual sample to this fold change is shown in Fig. 2b.

#### *Immunophenotyping using an 8-colour immunophenotype panel*

Data analysis of five concatenated files ($n = 5$) comparing the differences in immunophenotype between D0, D7 SR1, and D7 VC is demonstrated in Fig. 3. An equal number of events for each concatenated file was used in this analysis. The input population for the concatenated sample analysis was Lin-CD34+. Significant differences were observed between Lin-CD34+cells on D0 and D7. Manual gating of tSNE-CUDA islands was guided by the FlowSOM metaclustering analysis run within the tSNE-CUDA experiment. Identified populations were named according to pre-existing population nomenclature [29, 30, 38] as it pertained to the immunophenotypic profiles (Fig. 3b and c, only D0 and D7 SR1 shown). As our panel contains more colours than the
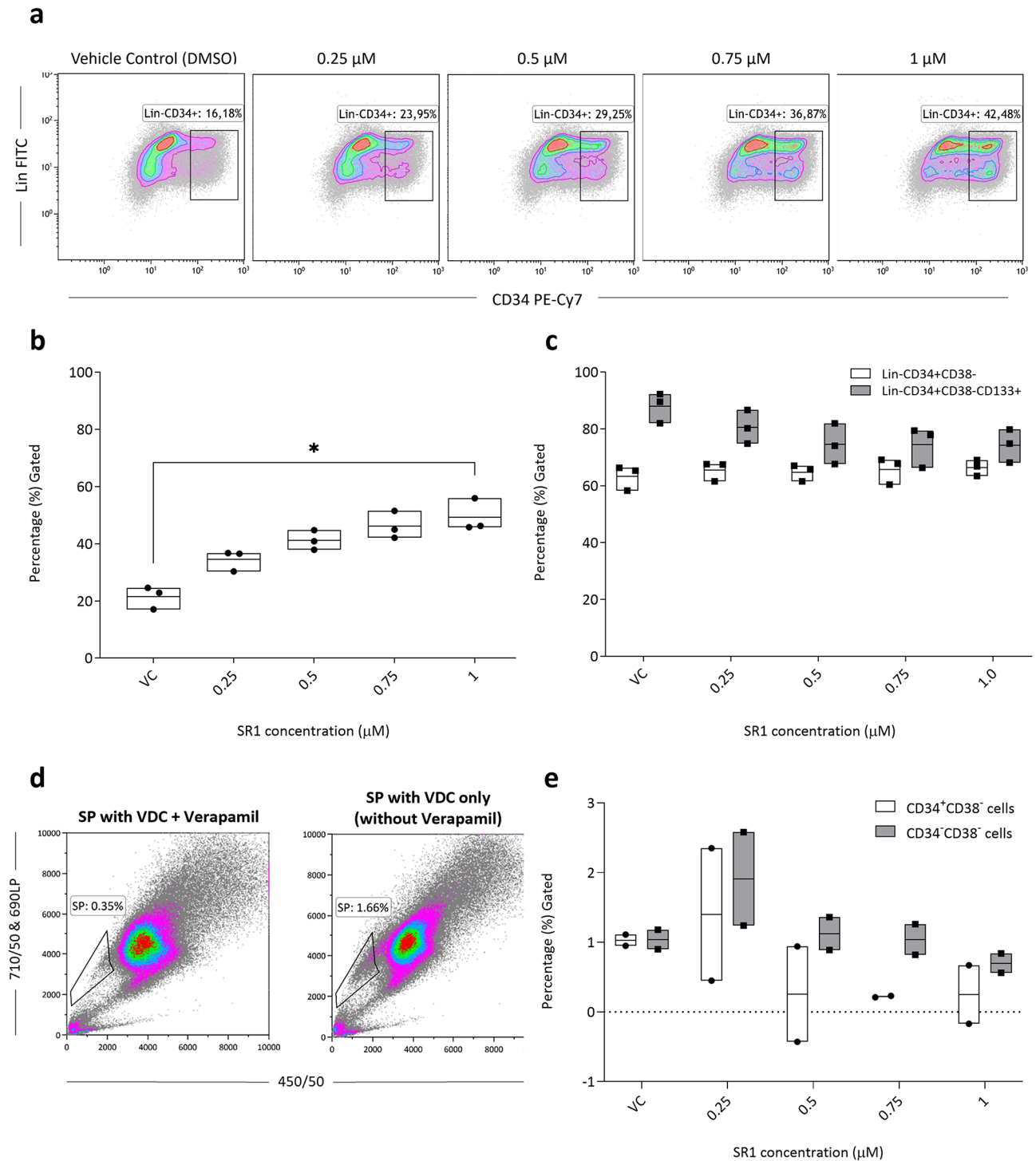
**Fig. 1** SR1 concentration optimisation. (**a**) A graphical illustration of flow cytometry density plots and minimum/maximum floating bar graphs indicating the (**b**) Lin-CD34+ and (**c**) Lin-CD38-CD34+ and Lin-CD38-CD34+CD133+ HSPC percentages present on D7 as the concentration of SR1 increases (*n* = 3). (**d**) A representation of the SP analysis, (i) VDC Violet with verapamil and (ii) VDC Violet without verapamil. (**e**) The percentage SP cells observed in the CD34+CD38- and CD34-CD38- populations after an 8-day expansion with different concentrations of SR1 (*n* = 2). Data is represented in minimum/maximum floating bar graphs with the solid horizontal line in each bar representing the mean. Significant differences are indicated as *($p < 0.05$)
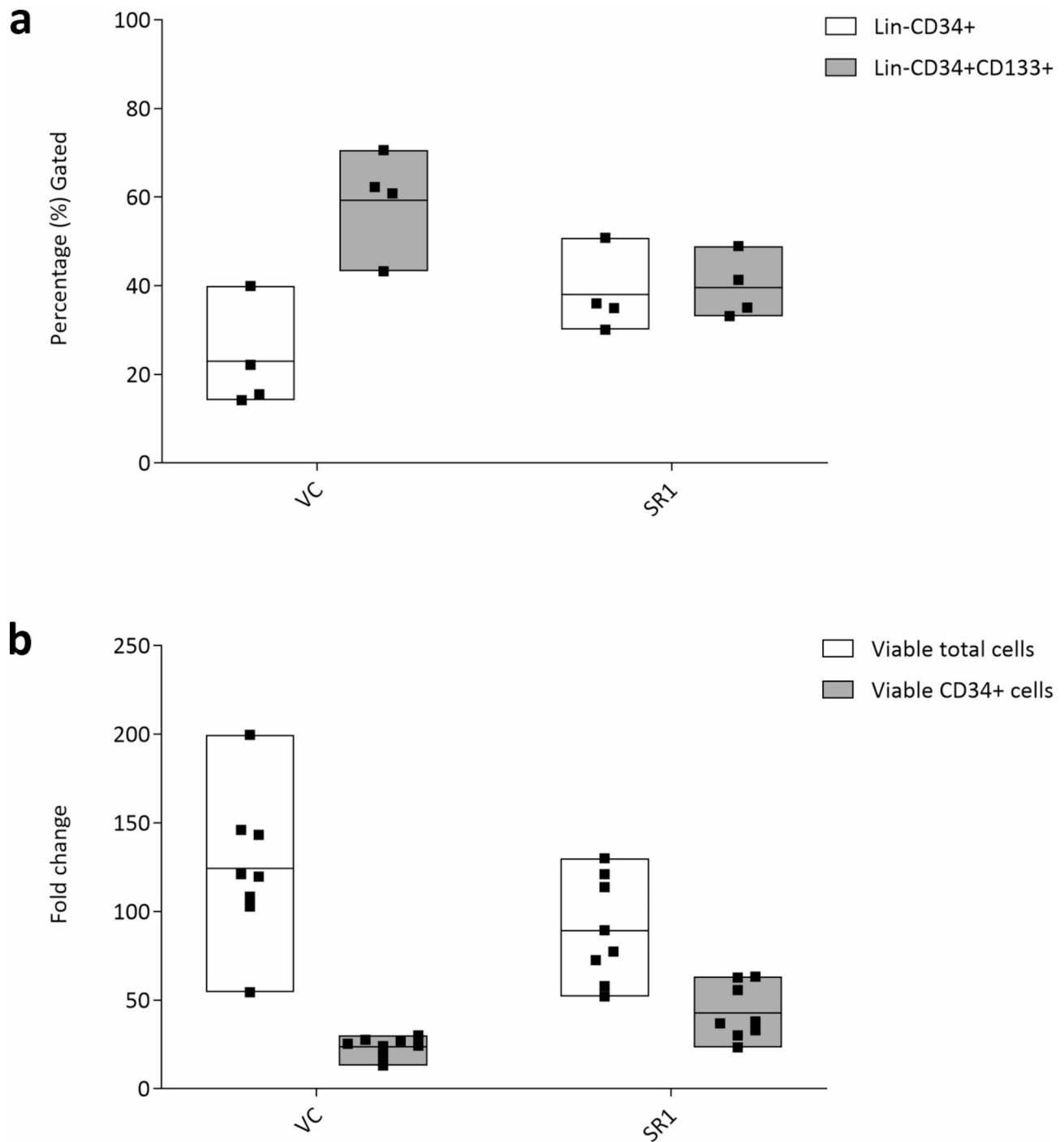
**Fig. 2** The effect of SR1 (1 µM) on CD34+ populations. The percentage (**a**) Lin-CD34+ and Lin-CD34+ CD133+ populations on D7 after expansion ($n=4$). (**b**) The fold change and mean fold change of total viable and CD34+ cells on D7 after expansion ($n=8$). Data is represented in minimum/maximum floating bar graphs with the solid horizontal line in each bar representing the mean

usual populations described, the term extended (Ext) was added to the population names. Population names and percentages are shown in Fig. 3b and c respectively, and the phenotypes of these distinct clusters are provided in Table 1. Six dominant clusters were identified on D0 and nine on D7. Overall, CD38 was expressed abundantly on D0, while the D7 populations, both in the presence and absence of SR1, were predominantly CD38- [31]. A very small CD49f+ seed population was seen on D0, making up 0.33% of the Lin-CD34+ population, with a marked increase in this population on D7 with SR1 (7.78% of the Lin-CD34+ population). The

**Fig. 3** (See legend on next page.)

(See figure on previous page.)

**Fig. 3** Concatenated D0 and D7 samples showing the differences in clusters present. (**a**) Shows the tSNE-CUDA map visualisation of concatenated D0 and D7 samples from the 8-colour immunophenotyping panel, coloured by expression of marker labelled above each plot as the z-dimension and plot scale indicated on the right. Significant expansion induced changes in clusters and phenotype are evident between D0 and D7. (**b**) Manual gating of the islands on the tSNE-CUDA was done using the FlowSOM metaclusters as guidance (MCs; not shown) and population names identified are shown in (b) while (**c**) shows relative percentages of the identified named populations. The tSNE-CUDA map shown in coloured by CD38 expression for concatenated D0 and D7 SR1 samples. To further describe the dynamic changes that occurs from D0 to D7, the manual gates guided by the FlowSOM MCs (not shown) were overlaid on the tSNE-CUDA map, illustrated in (**d**) for D0, D7 VC and D7 SR1). (**e**) Bar graphs showing the dramatic difference between populations present on D0 and D7, SR1 and VC, and relative abundance of each. (**f**) Event counts are shown in the tables below each bar graph

Lin-CD34+CD38+populations made up five of the six clusters on D0 and were further identified to be extended common myeloid progenitor (ExtCMP), -granulocyte-macrophage progenitor (ExtGMP), ExtGMP2, and -erythro-myeloid progenitor (ExtEMP) populations. The largest identified cluster was ExtCMP, which made up 41.19% of the Lin-CD34+population and is in keeping with what is known about this population in UCB on D0 [30]. This population additionally expressed both CD133 and CD117. In contrast, extended lymphoid primed multipotent progenitors (ExtLMPP) which give rise to multilymphoid progenitors (MLP) made up only 4.7%, and this population was the only D0 population on which CD117 was not expressed.

The D7 phenotype revealed an entirely different picture. Although many of the dominant clusters had very small seed populations which could be seen on D0, there were also new clusters present which were not present on D0. The two dominant clusters were ExtLMPP1 (63.02% in the VC and 25.58% in SR1) and a new population termed HSPC1 (18.12% in VC and 33.56% in SR1). The former, unlike its counterpart on D0 (Ext LMPP), expressed both CD90 and CD49f in small proportions and was brightly positive for CD117. The HSPC1 population is intriguing, as it lacked both CD38 and CD133, showed bright CD45RA expression, and included a small proportion which was CD90+. The highest CD90 expression was found in a distinct cluster present on D7 (CD90+). A minimal difference in its percentage between the VC and SR1 groups was observed. CD90 expression is associated with stemness [39] suggesting that the distinct CD90-expressing cluster observed on D7 represents primitive (immature) HSPCs. CD49f was not present on this CD90+population but rather formed its own unique cluster on D7 and was much more prominent in the presence of SR1 (7.78% versus 0.51% in the VC). Variable expression of CD90 was present within this CD49f population with intermediate/dim expression of CD133 and CD45RA. Variable expression here means that the presence and frequency of a specific cell surface marker varies among different cells within the same population. A second, very small CD90+population (CD90+(2)), making up 1.67% of the SR1 population and 0.39% of the VC, had a different phenotype from the first CD90+population, in that CD38 was present and CD133 was absent. This phenotype is in keeping with erythro-myeloid

progenitors (EMPs), except for the presence of CD90. The second HSC population (HSPC2) seen on D7 had a phenotype similar to HSPC1, except for CD45RA, which was variably expressed in HSPC2, and positive on HSPC1. HSPC2 also showed limited CD90 expression and clustered differently from HSPC1. Six of the clusters on D7 did not express CD38. Of the three clusters that did express CD38, namely D7ExtEMP, D7ExtGMP, and CD90+(2), all were more prominent in SR1 than in the VC. The absence of CD38 is evidence of a more immature HSPC population. The differences in the presence and abundance of these populations on D0 and D7 are illustrated in Fig. 3, which shows overlaid manually gated populations on the tSNE-CUDA (Fig. 3d), with corresponding bar graphs displaying event count per population (Fig. 3e). Statistical analysis of the different MCs identified by FlowSOM showed a statistically significant difference in all MCs between D0 and D7 as portrayed in the box plot in Fig. 4a.

To determine if any statistically significant differences occurred in sub-populations between treatment with SR1 and the VC on D7, a separate tSNE-CUDA experiment was performed using the five biological replicates ($n=5$) in each condition. A FlowSOM was run within this tSNE-CUDA experiment, and FlowSOM MCs were visualized on the tSNE-CUDA map. A Mann-Whitney U Test was applied to the generated FlowSOM MC box plots, shown in Fig. 4b, which identified three MCs indicating statistically significant differences between SR1 and VC. They were MC 13, 14, and 16. The three MCs in question were independently displayed on the FlowSOM MC dot overlays of one sample in Fig. 4c. Heat maps were then generated for these three MCs in the same sample to determine their unique phenotype (Fig. 4d). MC 13 was shown to have a phenotype similar to D7ExtGMP, MC 14 had similarities to D7ExtEMP, and MC 16 had a phenotype similar to CD90+(2) (see Table 1). These are the three CD38+populations on D7 which were more abundant in the presence of SR1, as shown in Table 1, corroborating the findings.

## Gene expression

Gene expression analysis was performed on D0 and 7-day-expanded (with and without SR1) CD34+HSPCs (Fig. 5a). Two UCB units, collected on the same day from two different donors, were pooled to obtain sufficient

**Table 1** Identified populations, their phenotypes and frequencies on D0 and D7 with (SR1) and without SR1 (VC)

| Population name | Phenotype | % D0 | % D7 VC | % D7 SR1 |
|---|---|---|---|---|
| ExtMPP | Lin-CD34+CD38-CD133+CD45RA-CD117+CD90-CD49f- | 5.42 | 0.01 | 0.01 |
| ExtCMP | Lin-CD34+CD38+CD133+CD45RA-CD117+CD90-CD49f- | 41.19 | 0 | 0.03 |
| ExtGMP | Lin-CD34+CD38+CD133vCD45RAdimCD117+CD90-CD49f- | 19.93 | 0.02 | 0 |
| ExtEMP | Lin-CD34+CD38+CD133-/dimCD45RA-CD117+CD90-CD49f- | 18.07 | 0.01 | 0.13 |
| ExtLMPP | Lin-CD34+CD38-CD133+CD45RAdimCD117-CD90-CD49f- | 4.7 | 0 | 0.01 |
| ExtGMP2 | Lin-CD34+CD38+CD133dimCD45RA+CD117vCD90-CD49f- | 8.16 | 0 | 0.15 |
| D7ExtEMP | Lin-CD34+CD38+CD133-CD45RA-CD117+CD90dimCD49f- | 0.08 | 1 | 9.31 |
| ExtLMPP1 | Lin-CD34+CD38-CD133+CD45RA+CD117+CD90vCD49fv | 0.04 | 63.02 | 25.58 |
| ExtLMPP2 | Lin-CD34+CD38dimCD133+CD45RA+CD117+CD90vCD49fdim | 0.01 | 3.15 | 1.34 |
| CD90+ | Lin-CD34+CD38-CD133+CD45RAvCD90+CD49f- | 0.01 | 4.32 | 3.77 |
| CD49f+ | Lin-CD34+CD38-CD133dimCD45RAdimCD117vCD90vCD49f+ | 0.33 | 0.51 | 7.78 |
| HSPC1 | Lin-CD34+CD38-CD133-CD45RA+CD117vCD90vCD49f- | 0.05 | 18.12 | 33.56 |
| HSPC2 | Lin-CD34+CD38-CD133-CD45RAvCD117+CD90vCD49f- | 0.01 | 5.94 | 9.89 |
| D7ExtGMP | Lin-CD34+CD38+CD133-/dimCD45RAvCD117+CD90vCD49fv | 0.01 | 0.79 | 3.05 |
| CD90+(2) | Lin-CD34+CD38+CD133-CD45RA-CD117dimCD90+CD49fv | 0.01 | 0.39 | 1.67 |

CD, cluster of differentiation; CMP, common myeloid progenitor; D0, day 0; D7, day 7; EMP, erythro-myeloid progenitor; Ext, extended; GMP, granulocyte-macrophage progenitor; HSPC, haematopoietic stem/progenitor cell; LMPP, lympho-myeloid primed progenitor; MPP, multipotent progenitor; SR1, stemregenin1; v, variable; VC, vehicle control

CD34+ HSPCs for subsequent RNA extraction and gene expression analysis. Three pooled samples, each consisting of two UCB units represented three biological repeats ($n=3$). Bulk gene expression analysis represents an average gene expression pattern of a population of cells. Figure 5b illustrates the conditions that were compared at the transcriptome level. Figure 5c shows two distinct clusters representing CD34+ HSPCs with different gene expression patterns through principal component analysis (PCA). A clear distinction between CD34+ HSPCs on D0 (blue) and D7 [with SR1 (purple) and VC (red)] was observed. Minimal gene expression differences were observed between cells expanded with and without SR1.

### CD34+ cells expanded with and without SR1

Two genes, namely cytochrome P450, family 1, subfamily B, polypeptide 1 (*CYP1B1*) and erythrocyte membrane protein band 4.1-like 3 *(EPB41L3)* (Table 2) were significantly downregulated in CD34+ cells expanded with SR1 when compared to the VC. No biological processes were associated with these genes.

### D7 vs. D0 CD34+ HSPCs

A total of 1037 and 1017 genes were differentially expressed in D7 CD34+ cells with and without SR1, respectively, when compared to CD34+ cells on D0. Of these, 470 genes were significantly upregulated and 567 were significantly downregulated in cells expanded with SR1 (Fig. 5b and Additional file 3: Table S1), while 489 genes were significantly upregulated and 528 were significantly downregulated in the VC (Fig. 5b and Additional file 3: Table S4). The heat map shows the gene expression patterns for D0 and D7 (SR1 and VC) CD34+ HSPCs (Fig. 6a). The volcano plots further show the significant

changes in gene expression with fold changes and statistical significance (Fig. 6b). GO classification revealed the biological processes enriched in the up- (Fig. 6c and Additional file 3: Tables S2 and S5) and downregulated (Fig. 6d and Additional file 3: Tables S3 and S6) gene sets.

## Discussion

The purpose of this study was to determine the effect of SR1 on immunophenotypic subsets and gene expression profiles of expanded CD34+ HSPCs as compared to a VC. These populations were then compared to HSPCs on D0, which are clinically used for HSCT and are known to engraft.

We first optimised the SR1 concentration for expansion, as previous studies used a variety of SR1 concentrations to expand HSPCs ex vivo [14, 15, 40, 41]. We found that 1 µM SR1 was the most effective; previous studies used concentrations ranging from 0.1 to 10 µM [14, 40]. CD34+ percentages were higher in SR1-expanded cultures compared to the VC (without SR1) and increased with higher concentrations of SR1, while the absolute number of viable cells was similar across the different concentrations. This indicates that SR1 increased the proportion and absolute number of CD34+ cells without affecting total cell number. This highlights the role of SR1 in promoting the expansion of CD34+ cells from UCB, which is in keeping with other studies [14, 15].

Immunophenotypic analysis revealed increased proportions of both CD34+CD38- and CD34+CD38+ populations as the concentration of SR1 increased. The CD34+CD38- fraction is known to be enriched in primitive HSPCs that have long-term repopulating potential, while CD34+CD38+ cells are enriched for short-term repopulating cells [15, 42]. On D7, an increase in the
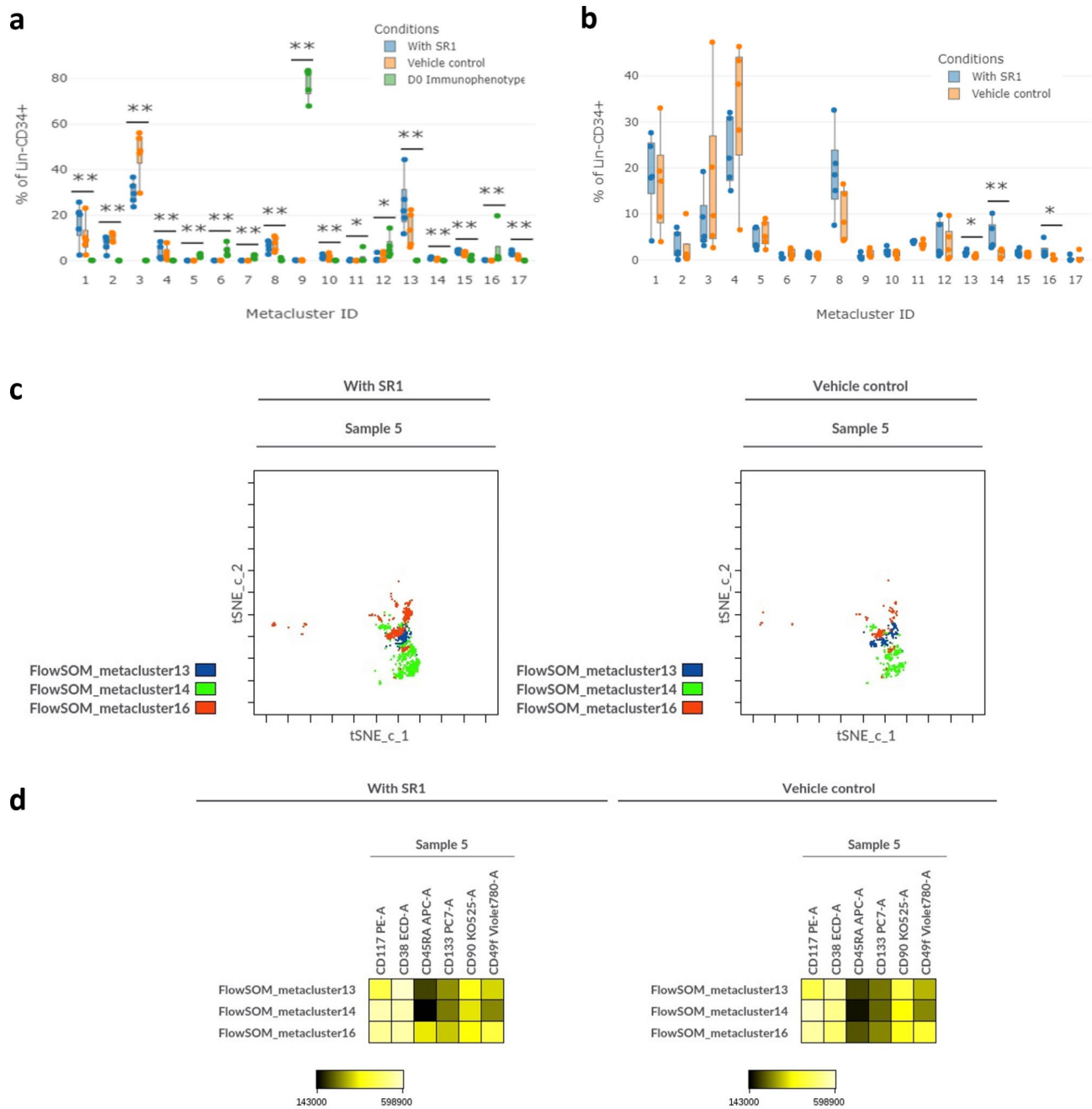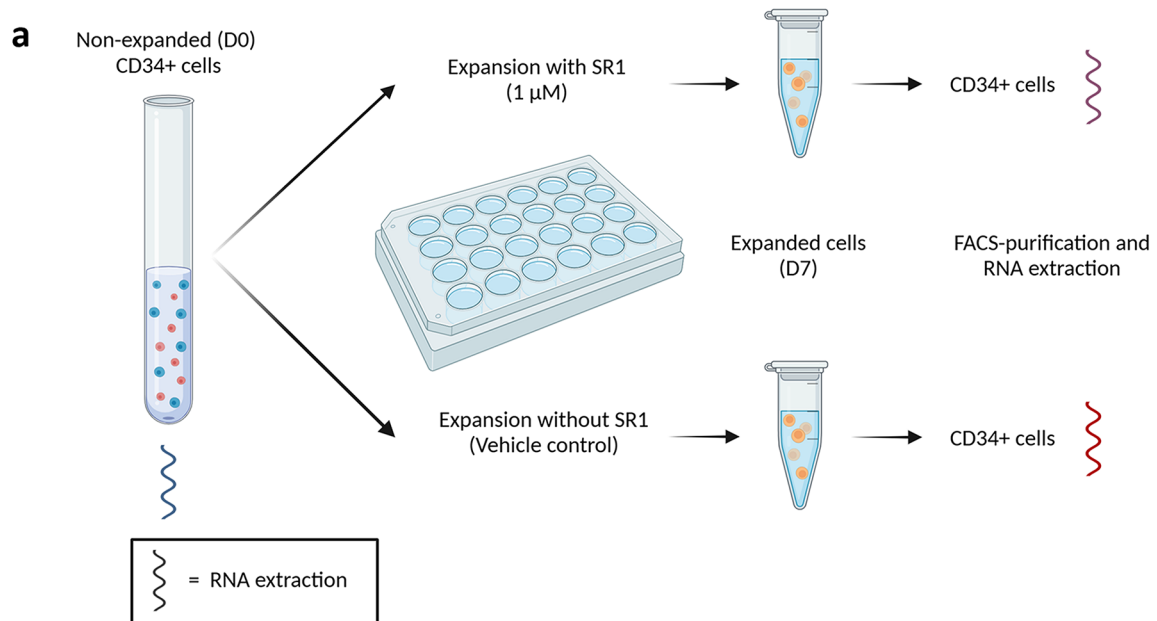
**Fig. 4** Statistical differences in Lin-C34+ sub-populations. The figure illustrates the differences in percentages of Lin-CD34+ sub-populations on D0 and D7 (with and without SR1) samples using Cytobank analysis software files from five individual donors (D0 and D7) were imported as individual files for statistical analysis (*n* = 5). (**a**) Significant differences are indicated on the boxplot as *(*p* < 0.05) and **(*p* < 0.01). Files from five individual donors (D0 and D7) were imported as individual files into Cytobank analysis software (*n* = 5). (**b**) A MC boxplot illustrating the differences in Lin-CD34+ sub-population percentages on D7 between cells expanded with and without SR1 (vehicle control, VC). Files were individually processed in Cytobank to determine the significance. Three sub-populations (MC 13, 14 and 16) were found to be significantly different between cells expanded with and without SR1. Significant differences are indicated on the boxplot as *(*p* < 0.05) and **(*p* < 0.01). (**c**) The FlowSOM MC dot overlay plots of one of the samples provides a visual representation of the differences in the three clusters of significance. (**d**) The FlowSOM MC heat maps shows the expression of the various markers on the three sub-populations that were found to be significantly different between the different conditions. Only one sample is shown for ease of visualisation

CD34+CD38- population was observed, which indicates a more primitive population of cells. However, this expanded population is not associated with SCID-repopulation capacity, as reported by Dorrell et al. [43].

Our findings are in line with other studies [14, 15], which also showed an increase in CD34+sub-populations when UCB-derived CD34+HSPCs were expanded ex vivo for five weeks with 1 µM SR1. Tao et al. [14] likewise showed

**a**



Non-expanded (D0) CD34+ cells

Expansion with SR1 (1 μM)

CD34+ cells

Expanded cells (D7)

FACS-purification and RNA extraction

Expansion without SR1 (Vehicle control)

CD34+ cells

= RNA extraction

**b**

| Comparisons | Upregulated | Downregulated |
|---|---|---|
| D7 VC vs D0 | 489 | 528 |
| D7 SR1 vs D0 | 470 | 567 |
| D7 SR1 vs VC | 2 | 2 |

**c**



PCA2 15,0%

PCA1 46,0%

PCA3 11,1%

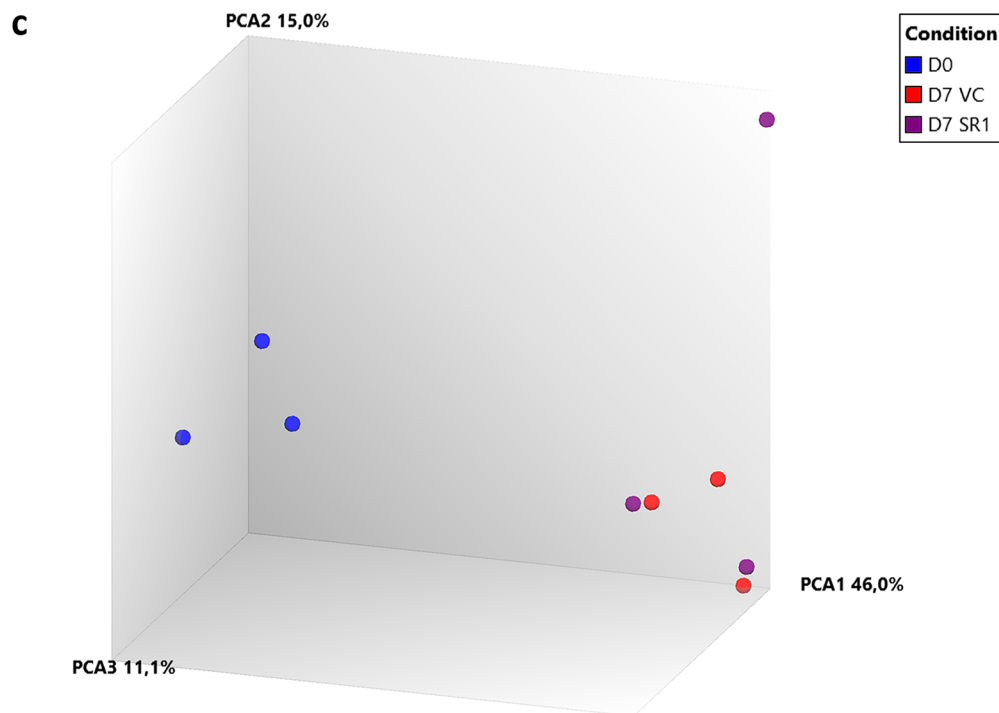Condition
- D0
- D7 VC
- D7 SR1

**Fig. 5** (See legend on next page.)

(See figure on previous page.)
**Fig. 5** Gene expression analysis. Experimental workflow for (**a**) RNA extractions and (**b**) comparisons for gene expression analysis. (**c**) A 3D plot of the first three principal components (PCs) of D0 (blue) and D7 CD34+ cells [with SR1 (purple) and VC (red)] (*n* = 3). Each dot represents a different time point/ condition. Figure 5a created with BioRender.com

that Lin-CD34+ cells expand in an SR1 concentration-dependent manner and observed a decrease in the more primitive and dormant CD34- population [33, 44–47] with higher concentrations of SR1 (1–5 μM). CD34-CD38- cells consistently showed higher SP percentages, further suggesting that they might be more primitive. Higher SR1 concentrations increased total CD34+ HSPC numbers but reduced primitive HSPCs. These concentrations likely contributed to changes in the phenotypic profiles of the HSPCs [47], including decreased dye efflux ability as cells mature [48].

Immunophenotyping on Cytobank analysis software using an 8-colour panel was able to provide important new insights into HSPC phenotyping in an unbiased manner. A very small percentage of Lin-CD34+CD38- cells were present on D0 in keeping with other studies [49], whilst on D7, the majority of cell clusters were Lin-CD34+CD38-. Pranke et al. [49]. found similar results after a 7-day culture with TPO, FLT-3, and SCF but in contrast to our findings, their CD34+ percentages decreased from 93.3% on D0 (purified CD34+ culture plating) to 10.9% on D7. Our higher mean CD34+ percentages on D7 both in VC and SR1, are likely due to the increased number of cytokines (FLT3L, SCF, TPO, IL-3, and G-CSF) in addition to SR1. However, the conclusion reached by these authors [49] is similar to ours, namely that differentiation and thus loss of CD34 marker expression occurs during culture. This differentiation likely affects the less primitive D0 CD34+CD38+ population more than their CD34+CD38- counterparts, which undergo more self-renewal [49] in culture and are therefore more abundant. It is thus probable that the Lin-CD34+CD38- populations present on D7 stem from the initial D0 populations as well as self-renewal of the MPP population.

The "Revised model of early haematopoiesis" [38] identifies the MPP as a cell that has lost its self-renewal capacity and is CD34+CD38-CD133+CD45RA-CD90-. However, studies have shown that this population is capable of long-term engraftment in mice [50, 51], although it is less efficient than Lin-CD34+CD45RA-CD90+ (HSCs) cells [52]. The MPP population [30, 38, 51] is clearly visible on the tSNE plots on D0 with bright CD117 expression. Our study showed, similar to others [38], that the D0 CD34+ population is predominantly CD133+, which has been found to have greater colony-forming potential compared to the same population in peripheral blood or bone marrow [28]. Engraftment in mice has also been shown to be possible only when CD133 is expressed [38].

Our study revealed some distinct differences on the D7 immunophenotype in the presence and absence of SR1. SR1 favoured the development of CD49f, EMP (D7ExtEMP), HSPC1, and HSPC2 populations while the VC showed a marked increase in LMPP (ExtLMPP1 and 2). CD49f expression in SR1-treated cells on D7 is considerably brighter than in the VC with concurrent dim CD90 expression, and up to 80% of single CD34+CD90+CD49f+ HSPCs have also been found to have colony forming potential [27]. This indicates that SR1 potentially favours the expansion of a potent HSPC subtype that may aid engraftment, especially since even the CD90-CD49f+ population has been found to possess long-term engraftment potential [50]. According to Notta et al., up to 70% of CD90+ HSPCs express CD49f [50], but we were not able to quantify this on our tSNE plot. Co-expression of CD90 and CD49f in the Lin-CD34+ population (Lin-CD34+CD90+CD49f+) has been shown to constitute a rare but potent HSPC subtype, which is enriched for true HSCs that have the ability to engraft NOD-SCID mice and can be distinguished from MPPs [50]. Evidence suggests that the MPP population has the potential to increase expression of CD90 and therefore to engraft well [50], albeit to a lesser extent than the CD90+CD49f+ population. Bari et al. [52] showed that a significantly increased proportion of the Lin-CD34+CD90+CD49f+ sub-population is present after expansion with a small molecule (C7), and transplantation of expanded cells leads to rapid engraftment in NSG mice. These findings are further supported by our data in that the HSC phenotype forms a sub-population of the HSPC2 population found on D7 (HSPC2 = MPP sub-population + HSC sub-population) with a higher prevalence in SR1.

The most prominent population in SR1 expanded cultures was HSPC1. This population is predominantly CD38-CD133-CD45RA+ with variable expression of

**Table 2** Significantly downregulated genes in CD34+ HSPCs expanded with SR1 for 7 days (*n* = 3)

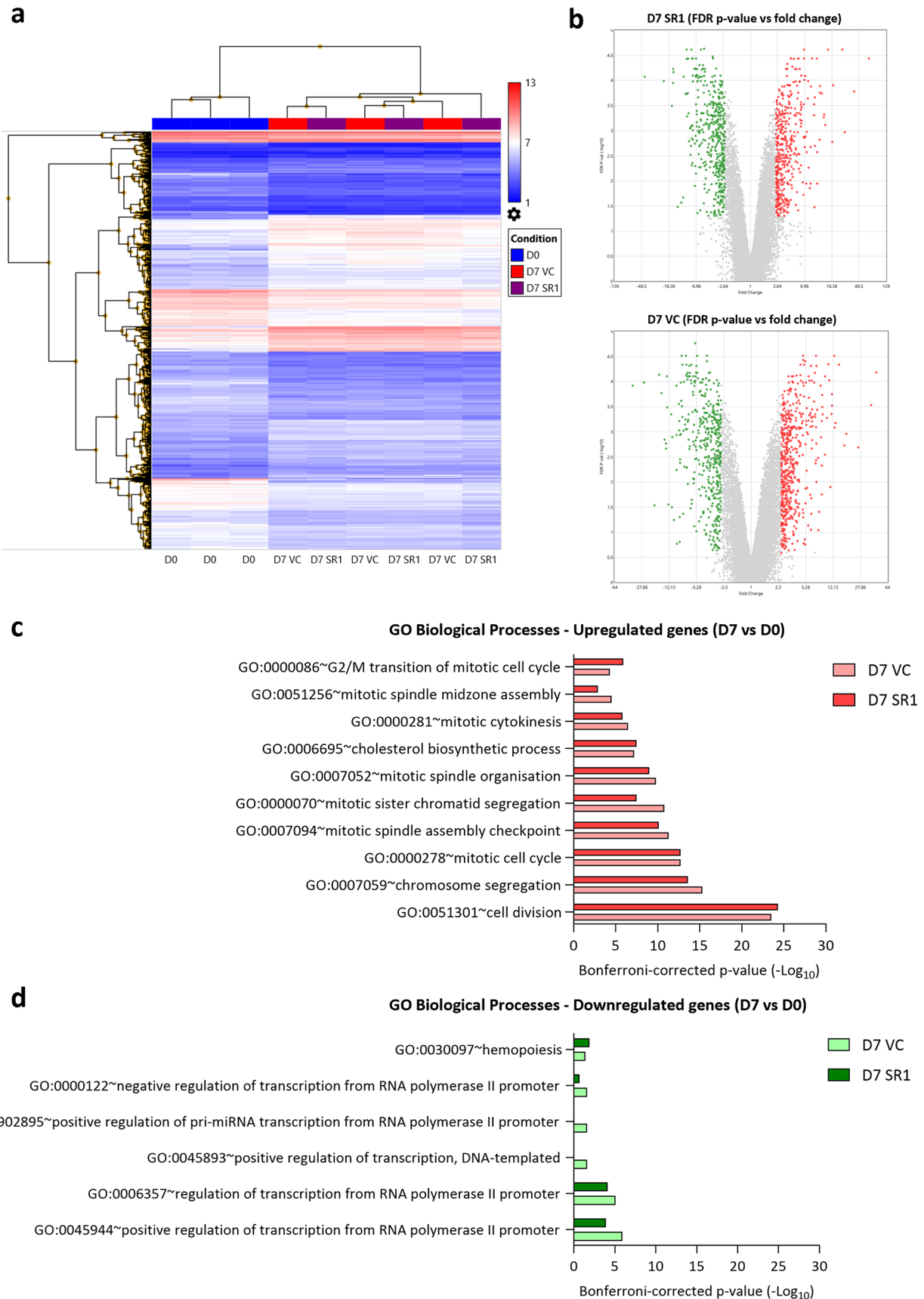| Gene | Gene symbol | Fold change | *P*-value | FDR *P*-value |
|---|---|---|---|---|
| Cytochrome P450, family 1, subfamily B, polypeptide 1 | *CYP1B1* | -9.38 | 1.98E-07 | 0.0096 |
| Erythrocyte membrane protein band 4.1-like 3 | *EPB41L3* | -2.57 | 2.45E-05 | 0.5916 |

FDR, False detection rate

**Fig. 6** (See legend on next page.)

(See figure on previous page.)

**Fig. 6** Differentially up- and downregulated genes. (**a**) A heat map showing the gene expression patterns on D7 (top red and purple bar) and D0 (top blue bar). (**b**) A volcano plot showing significant up- (red) and downregulated (green) genes between expanded D7 (SR1 and VC) and D0 CD34+ cells. GO classification revealed biological processes (Bonferroni-corrected p-value < 0.05) enriched for significantly (**c**) up- and (**d**) downregulated genes in D7 (SR1 and VC) vs. D0 CD34+ HSPCs

CD90. This phenotype may lean towards an LMPP population due to the presence of CD45RA. On the other hand, the LMPP population described by Görgens et al., which is both positive for CD45RA and CD133, is found in 63.02% of the VC and 25.58% of SR1 on D7 [38]. This shows that in the absence of a molecule preventing differentiation of CD34+ HSPCs (VC), LMPPs dominate, which in turn will give rise to multipotent lymphoid progenitors (MLPs) and/or GMPs [28, 38]. On D7, the ExtLMPP1 population contains CD45RA+CD90- and CD45RA+CD90+ populations. The former has been shown to have poor engraftment potential in mice as well as poor colony forming potential [51]; however, this study did not include CD133 when determining engraftment. In the absence of CD10, it was not easy to differentiate LMPPs from MLPs, but GMPs were prominent on D0 (17.87%) with much lower percentages seen on D7. On D7, an EMP population (D7ExtEMP) showed a marked increase in the presence of SR1 compared to VC (9.31% vs. 1%). EMPs arise from the classic MPP, which gives rise to eosinophils/basophils and the MEPs.

The effect of SR1 on HSPC gene expression has previously been evaluated for shorter culture periods [15, 31]. Boitano et al. [15] have shown downregulation of AhR pathway-related genes, aryl hydrocarbon receptor repressor (*AHRR)* and heat-shock protein 90α (*HSP90AA1),* after 48 h with SR1, which we did not observe on D7. This might suggest that the initial action of SR1 on the above-mentioned genes returns to normal if SR1 is not continually added to the culture medium. In our study, SR1 significantly reduced *CYP1B1* ($P = 8.15\text{E-06}$) and *EPB41L3* ($P = 1.44\text{E-05}$) expression on D7. *CYP1B1* is a target of AhR and its downregulation suggests that SR1 antagonises AhR in HSPCs. Downregulation of *CYP1B1* was also observed after 48 h [15] and 4 days [40] of expansion with SR1 in other studies. However, our study observed a greater decrease in *CYP1B1*, which may be due to the longer expansion period. This suggests a long-lasting effect of SR1 on *CYP1B1*. The exact role of *EPB41L3* in HSPCs is unknown, but it is a potential tumour suppressor gene [53]. Boitano et al. [15] have shown that the effect of SR1 is reversible. It is therefore possible that these genes might return to normal when SR1 is removed. However, our study did not confirm this at the transcriptome level.

Our study showed limited changes in gene expression in HSPCs expanded with SR1 for 7-days when compared to cells grown under the same conditions that were not exposed to SR1. The gene expression profiles between D0 and D7 CD34+ HSPCs were however noticeably different. GO classification revealed that upregulated genes in D7 vs. D0 CD34+ HSPCs were enriched for processes such as cell division and mitosis. Minimal changes were observed between D7 CD34+ HSPCs with and without SR1, which suggests that the observed differences between D0 and D7 CD34+ HSPCs are likely due to the added cytokines or the expansion process itself, which are likely to drive the processes identified by GO analysis. Downregulated processes included regulation of transcription from RNA polymerase and haematopoiesis. Despite these transcriptional differences observed between D0 and D7 CD34+ HSPCs, studies have shown successful engraftment of SR1-expanded HSPCs in murine models [15, 41], and clinical trials are assessing their use in HSCT together with non-expanded UCB units [9].

Although we did not perform functional assays, studies have shown that SR1-expanded HSPCs have colony-forming potential [15, 41]. Secondary transplantation studies in mice showed improved engraftment of SR1-expanded HSPCs in primary and secondary recipients [15, 41]. Immunophenotype analysis suggests that certain subsets of CD34+ HSPCs may have greater engraftment potential, paving the way for future engraftment studies.

## Conclusion

This study demonstrates that SR1 increased CD49f expression, with two unique HSPC populations being identified. This suggests SR1 may potentially select for more potent HSPC subsets, which in addition to increased CD34+ HSPC numbers, may improve engraftment potential post-expansion. This would need to be verified in vivo in pre-clinical animal models to determine the most potent sub-population. This study further revealed that SR1 has a minimal effect on the transcriptome of 7-day expanded CD34+ HSPCs when compared to cells expanded without SR1, with only two genes being downregulated in the former. In contrast, the transcriptome of cytokine expanded CD34+ cells on D7 markedly differed from D0 CD34+ cells. GO classification of differentially expressed genes suggests that the gene expression changes are related to cell division. With expansion of UCB units gaining favour, and studies showing the potential of a stand-alone graft, we may be able to reach a point where CD34+ cell number becomes redundant in favour of the selection of a particular subtype of HSPCs, which at low numbers are able to reconstitute the bone marrow following engraftment.

## Limitations

The findings in this study should be interpreted with caution as they are limited by the lack of functional studies, including colony-forming unit assays and engraftment studies, as well as the small sample size used for gene expression analysis. Furthermore, the addition of CD10 would improve the classification of the clusters observed.

## Abbreviations

| | |
|---|---|
| 7-AAD | 7-Actinomycin-D |
| ACF | Animal component free |
| AhR | Aryl hydrocarbon receptor |
| ANOVA | Analysis of variance |
| AOF | Animal origin free |
| APC | Allophycocyanin |
| CD | Cluster of differentiation |
| CMP | Common myeloid progenitor |
| Co2 | Carbon Dioxide |
| CYP1B1 | Cytochrome P450 family 1 subfamily B member 1 |
| D0 | Day 0 |
| D7 | Day 7 |
| DAVID | The Database for Annotation, Visualization, and Integrated Discovery |
| DMSO | Dimethyl sulfoxide |
| DNA | Deoxyribonucleic acid |
| ECD | Phycoerythrin-Texas Red |
| EDTA | Ethylenediaminetetraacetic acid |
| EMP | Erythro-myeloid progenitor |
| EPB41L3 | Erythrocyte membrane protein band 4.1 like 3 |
| Ext | Extended |
| FDR | False discovery rate |
| FITC | Fluorescein isothiocyanate |
| FLT3L | FMS-like tyrosine kinase 3 ligand |
| G-CSF | Granulocyte colony stimulation factor |
| GEO | Gene expression omnibus |
| GMP | Granulocyte-macrophage progenitor |
| GO | Gene ontology |
| HIV | Human immunodeficiency virus |
| HLA | Human leukocyte antigen |
| HSCT | Haematopoietic stem cell transplantation |
| HSPC | Haematopoietic stem and progenitor cell |
| IL | Interleukin |
| Lin | Lineage cocktail |
| LMPP | Lympho-myeloid primed progenitor |
| NAM | Nicotinamide |
| NCBI | National Centre for Biotechnology Information |
| MNC | Mononuclear cells |
| MPP | Multipotent progenitor |
| NH4Cl | Ammonium Chloride |
| PBS | Phosphate buffered saline |
| PCA | Principal component analysis |
| PE | Phycoerythrin |
| PE-Cy7 | Phycoerythrin-Cyanine 7 |
| Rpm | rounds per minute |
| SB | Super Bright |
| SCF | Stem cell factor |
| SD | Standard deviation |
| SP | Side population |
| SR1 | StemRegenin1 |
| RNA | Ribonucleic acid |
| TAC | Transcriptome Analysis Console |
| tSNE | t-distributed Stochastic Neighbour Embedding |
| TPO | Thrombopoietin |
| UCB | Umbilical cord blood |
| UCBT | Umbilical cord blood transplantation |
| v | Variable |
| VC | Vehicle control |
| VDC | Vybrant DyeCycle |

## Supplementary Information

The online version contains supplementary material available at https://doi.org/10.1186/s13287-024-03895-x.

Supplementary Material 1

Supplementary Material 2

Supplementary Material 3

Supplementary Material 4

## Author contributions

JM: Conception and design, collection and/or assembly of data, data analysis and interpretation, manuscript writing: original draft, manuscript editing. CLH: Conception and design, collection and/or assembly of data, data analysis and interpretation, manuscript writing: original draft, manuscript editing. VS: Data analysis and interpretation, editing and final approval of the manuscript. CD: Conception and design, collection and/or assembly of data, data analysis and interpretation, editing and final approval of manuscript. MAA: Collection and/or assembly of data, data analysis and interpretation, final approval of manuscript. MSP: Conception and design, PhD supervisor, financial support, administrative support, editing and final approval of manuscript.

## Data availability

The flow cytometry data used and/or analysed during the current study are available from the corresponding author on request. The gene expression data used and analysed during the current study are available in the GEO repository [accession number GSE146810 in https://www.ncbi.nlm.nih.gov/geo/].

## Declarations

### Ethics approval and consent to participate

This study was conducted at the Institute for Cellular and Molecular Medicine (ICMM), Department of Immunology, University of Pretoria. Approval was granted for two projects titled "Hematopoietic stem and progenitor cell heterogeneity and susceptibility to HIV-1" in 2014 and "Characterisation of umbilical cord blood derived haematopoietic stem and progenitor cells from HIV exposed infants that are HIV negative at birth" in 2020 by the Faculty of Health Sciences Research Ethics Committee. The protocol numbers are 410/2014 (30 October 2014) and 102/2020 (28 July 2020), respectively. Additionally, approval was obtained from the Research Operations Committee of the private hospital group concerned with the approval numbers UNIV-2014-0058 and UNIV-2021-0007.

### Consent for publication

Not applicable.

### Competing interests

The authors declare the following: Michael S. Pepper has received research grant funding from the South African Medical Research Council, the Bill and Melinda Gates Foundation, the South African National Research Foundation and the National Health Laboratory Service Research Trust, and the Wellcome Trust. He is a co-founder and non-remunerated Board Member of Antion Biosciences. Candice L. Hendricks is a non-remunerated board member of DKMS Africa, a not-for-profit organisation. The authors used products/services from a commercial company that Voula Stivaktas is affiliated with (Beckman Coulter).

## Author details
[1]Institute for Cellular and Molecular Medicine, Department of Medical Immunology, South African Medical Research Council (SAMRC) Extramural Unit for Stem Cell Research and Therapy, Faculty of Health Sciences, University of Pretoria, Pretoria, South Africa
[2]Beckman Coulter Life Sciences, Centurion, South Africa
[3]Department of Oral and Maxillofacial Pathology, Faculty of Health Sciences, University of Pretoria, Pretoria, South Africa

## References
1. Ballen KK, Gluckman E, Broxmeyer HE. Umbilical cord blood transplantation: the first 25 years and beyond. Blood [Internet]. 2013;122:491–8. http://www.bloodjournal.org/cgi/doi/https://doi.org/10.1182/blood-2013-02-453175
2. Rafii H, Garnier F, Ruggeri A, Ionescu I, Ballot C, Bensoussan D, et al. Umbilical cord blood transplants facilitated by the French cord blood banks network. On behalf of the Agency of Biomedicine, Eurocord and the French society of bone marrow transplant and cell therapy (SFGM-TC). Bone Marrow Transpl. 2021;56:2497–509.
3. Inoue H, Yasuda Y, Hattori K, Shimizu T, Matsumoto M, Yabe M, et al. The kinetics of Immune reconstitution after cord blood transplantation and selected cd34 + stem cell transplantation in children: comparison with bone marrow transplantation. Int J Hematol. 2003;77:399–407.
4. Linder KA, McDonald PJ, Kauffman CA, Revankar SG, Chandrasekar PH, Miceli MH. Infectious complications after umbilical cord blood transplantation for hematological malignancy. Open Forum Infect Dis. 2019;6.
5. Dessels C, Alessandrini M, Pepper MS. Factors influencing the umbilical cord blood stem cell industry: an Evolving Treatment Landscape. Stem Cells Transl Med. 2018;7:643–50.
6. Zimran E, Papa L, Hoffman R. Ex vivo expansion of hematopoietic stem cells: finally transitioning from the lab to the clinic. Blood Rev. 2021;50:100853.
7. Delaney C, Heimfeld S, Brashem-Stein C, Voorhies H, Manger RL, Bernstein ID. Notch-mediated expansion of human cord blood progenitor cells capable of rapid myeloid reconstitution. Nat Med. 2010;16:232–6.
8. Horwitz ME, Chao NJ, Rizzieri DA, Long GD, Sullivan KM, Gasparetto C, et al. Umbilical cord blood expansion with nicotinamide provides long-term multilineage engraftment. J Clin Invest. 2014;124:3121–8.
9. Wagner JE, Brunstein CG, Boitano AE, DeFor TE, McKenna D, Sumstad D, et al. Phase I/II trial of StemRegenin-1 expanded umbilical cord blood hematopoietic stem cells supports testing as a stand-alone graft. Cell Stem Cell. 2016;18:144–55.
10. Ueda T, Tsuji K, Yoshino H, Ebihara Y, Yagasaki H, Hisakawa H, et al. Expansion of human NOD / SCID-repopulating cells by stem cell factor, Flk2 / Flt3 ligand, thrombopoietin, IL-6, and soluble IL-6 receptor. J Clin Invest. 2000;105:1013–21.
11. Bordeaux-Rego P, Luzo A, Costa FF, Olalla Saad ST, Crosara-Alberto DP. Both interleukin-3 and interleukin-6 are necessary for better ex vivo expansion of CD133 + cells from umbilical cord blood. Stem Cells Dev [Internet]. 2010;19:413–22. http://www.ncbi.nlm.nih.gov/pubmed/19656071
12. Norkin M, Lazarus HM, Wingard JR. Umbilical cord blood graft enhancement strategies: has the time come to move these into the clinic? Bone Marrow Transpl. 2013;48:884–9.
13. Peled T, Shoham H, Aschengrau D, Yackoubov D, Frei G, Rosenheimer GN et al. Nicotinamide, a SIRT1 inhibitor, inhibits differentiation and facilitates expansion of hematopoietic progenitor cells with enhanced bone marrow homing and engraftment. Exp Hematol [Internet]. 2012;40:342–355.e1. https://linkinghub.elsevier.com/retrieve/pii/S0301472X11005972
14. Tao L, Togarrati PP, Choi KD, Suknuntha K. Stemregenin 1 selectively promotes expansion of multipotent hematopoietic progenitors derived from human embryonic stem cells. J Stem Cells Regen Med. 2017;13:P75–9.
15. Boitano AE, Wang J, Romeo R, Bouchez LC, Parker AE, Sutton SE et al. Aryl hydrocarbon receptor antagonists promote the expansion of human hematopoietic stem cells. Science [Internet]. 2010;329:1345–8. http://www.ncbi.nlm.nih.gov/pubmed/20688981
16. Thordardottir S, Hangalapura BN, Hutten T, Cossu M, Spanholtz J, Schaap N, et al. The aryl hydrocarbon receptor antagonist StemRegenin 1 promotes human plasmacytoid and myeloid dendritic cell development from CD34 + hematopoietic progenitor cells. Stem Cells Dev. 2014;23:955–67.
17. Singh J, Chen ELY, Xing Y, Stefanski HE, Blazar BR, Zúñiga-Pflücker JC. Generation and function of progenitor T cells from StemRegenin-1–expanded CD34 + human hematopoietic progenitor cells. Blood Adv. 2019;3:2934–48.
18. Zhu X, Sun Q, Tan W, Cai H. Reducing TGF-β1 cooperated with StemRegenin 1 promoted the expansion ex vivo of cord blood CD34 $^+$ cells by inhibiting AhR signalling. Cell Prolif. 2021;54.
19. Lim HJ, Jang WB, Rethineswaran VK, Choi J, Lee EJ, Park S, et al. StemRegenin-1 attenuates endothelial progenitor cell senescence by regulating the AhR pathway-mediated CYP1A1 and ROS generation. Cells. 2023;12:2005.
20. Ikuta T, Eguchi H, Tachibana T, Yoneda Y, Kawajiri K. Nuclear localization and export signals of the human aryl hydrocarbon receptor. J Biol Chem. 1998;273:2895–904.
21. Cohen S, Roy J, Lachance S, Marinier A, Roy D-C, Delisle J-S, et al. Single UM171 expanded cord blood transplant is feasible, safe, and permits transplantation of Better HLA Matched Cords with very low transplant related mortality. Blood. 2017;130:658–658.
22. Cohen S, Roy J, Lachance S, Delisle JS, Marinier A, Busque L, et al. Hematopoietic stem cell transplantation using single UM171-expanded cord blood: a single-arm, phase 1–2 safety and feasibility study. Lancet Haematol. 2020;7:e134–45.
23. Gragert L, Eapen M, Williams E, Freeman J, Spellman S, Baitty R, et al. HLA Match likelihoods for hematopoietic stem-cell grafts in the U.S. Registry. N Engl J Med. 2014;371:339–48.
24. Barker JN, Weisdorf DJ, DeFor TE, Blazar BR, McGlave PB, Miller JS et al. Transplantation of 2 partially HLA-matched umbilical cord blood units to enhance engraftment in adults with hematologic malignancy. Blood [Internet]. 2005;105:1343–7. http://www.ncbi.nlm.nih.gov/pubmed/15466923
25. Viljoen IM, Hendricks CL, Mellet J, Pepper MS. Perspectives on establishing a public cord blood inventory in South Africa. Cytotherapy. 2021;23:548–57.
26. Nikiforow S, Ritz J. Dramatic expansion of HSCs: new possibilities for HSC transplants? Cell Stem Cell. 2016;18:10–2.
27. Belluschi S, Calderbank EF, Ciaurro V, Pijuan-Sala B, Santoro A, Mende N et al. Myelo-lymphoid lineage restriction occurs in the human haematopoietic stem cell compartment before lymphoid-primed multipotent progenitors. Nat Commun. 2018;9.
28. Radtke S, Görgens A, Kordelas L, Schmidt M, Kimmig KR, Köninger A, et al. CD133 allows elaborated discrimination and quantification of haematopoietic progenitor subsets in human haematopoietic stem cell transplants. Br J Haematol. 2015;169:868–78.
29. Dmytrus J, Matthes-Martin S, Pichler H, Worel N, Geyeregger R, Frank N, et al. Multi-color immune-phenotyping of CD34 subsets reveals unexpected differences between various stem cell sources. Bone Marrow Transpl. 2016;51:1093–100.
30. Mantri S, Reinisch A, Dejene BT, Lyell DJ, DiGiusto DL, Agarwal-Hashmi R, et al. CD34 expression does not correlate with immunophenotypic stem cell or progenitor content in human cord blood products. Blood Adv. 2020;4:5357–61.
31. Psatha N, Georgolopoulos G, Phelps S, Papayannopoulou T. Brief report: a Differential Transcriptomic Profile of Ex vivo expanded adult human hematopoietic stem cells empowers them for Engraftment Better than their surface phenotype. Stem Cells Transl Med. 2017;6:1852–8.
32. Jackson CS, Durandt C, van Janse I, Praloran V, de la Brunet P, Pepper MS. Targeting the aryl hydrocarbon receptor nuclear translocator complex with DMOG and Stemregenin 1 improves primitive hematopoietic stem cell expansion. Stem Cell Res [Internet]. 2017;21:124–31. https://doi.org/10.1016/j.scr.2017.04.007
33. Goodell MA, Rosenzweig M, Kim H, Marks DF, DeMaria M, Paradis G et al. Dye efflux studies suggest that hematopoietic stem cells expressing low or undetectable levels of CD34 antigen exist in multiple species. Nat Med [Internet]. 1997;3:1337–45. http://www.ncbi.nlm.nih.gov/pubmed/9396603
34. Huang DW, Sherman BT, Lempicki RA. Systematic and integrative analysis of large gene lists using DAVID bioinformatics resources. Nat Protoc. 2009;4:44–57.
35. Pearce DJ, Bonnet D. The combined use of Hoechst efflux ability and aldehyde dehydrogenase activity to identify murine and human hematopoietic stem cells. Exp Hematol [Internet]. 2007;35:1437–46. https://linkinghub.elsevier.com/retrieve/pii/S0301472X07003530
36. Storms RW, Goodell MA, Fisher A, Mulligan RC, Smith C. Hoechst dye efflux reveals a novel CD7(+)CD34(-) lymphoid progenitor in human umbilical cord blood. Blood [Internet]. 2000;96:2125–33. http://www.ncbi.nlm.nih.gov/pubmed/10979957

37. Guo Y, Follo M, Geiger K, Lübbert M, Engelhardt M. Side-Population Cells from Different Precursor Compartments. J Hematother Stem Cell Res [Internet]. 2003;12:71–82. https://www.liebertpub.com/doi/10.1089/15258160332121015 4

38. Görgens A, Radtke S, Möllmann M, Cross M, Dürig J, Horn PA et al. Revision of the Human Hematopoietic Tree: Granulocyte Subtypes Derive from Distinct Hematopoietic Lineages. Cell Rep [Internet]. 2013;3:1539–52. https://linkinghub.elsevier.com/retrieve/pii/S2211124713002076

39. Mantri S, Rao EV, Jena PK, Mohapatra PC. Association of CD34 + and CD90 + stem cells of cord blood with neonatal factors: a cross-sectional study. Indian J Pediatr. 2016;83:114–9.

40. Koide R, Kulkeaw K, Tanaka Y, Swain A, Nakanishi Y, Sugiyama D. Aryl Hydrocarbon Receptor Antagonist StemRegenin 1 Promotes the Expansion of Human Promyelocytic Leukemia Cell Line, NB4. Anticancer Res [Internet]. 2016;36:3635–43. http://www.ncbi.nlm.nih.gov/pubmed/27354634

41. Jackson CS, Durandt C, Janse van Rensburg I, Praloran V, de la Brunet P, Pepper MS. Targeting the aryl hydrocarbon receptor nuclear translocator complex with DMOG and Stemregenin 1 improves primitive hematopoietic stem cell expansion. Stem Cell Res [Internet]. 2017;21:124–31. https://linkinghub.elsevier.com/retrieve/pii/S1873506117300739

42. Zonari E, Desantis G, Petrillo C, Boccalatte FE, Lidonnici MR, Kajaste-Rudnitski A et al. Efficient Ex Vivo Engineering and Expansion of Highly Purified Human Hematopoietic Stem and Progenitor Cell Populations for Gene Therapy. Stem Cell Reports [Internet]. 2017;8:977–90. https://doi.org/10.1016/j.stemcr.2017.02.010

43. Dorrell C, Gan OI, Pereira DS, Hawley RG, Dick JE. Expansion of human cord blood CD34 + CD38 – cells in ex vivo culture during retroviral transduction without a corresponding increase in SCID repopulating cell (SRC) frequency: dissociation of SRC phenotype and function. Blood. 2000;95:102–10.

44. Andreeva ER, Andrianova IV, Gornostaeva AN, Gogiya BSh, Buravkova LB. Evaluation of committed and primitive cord blood progenitors after expansion on adipose stromal cells. Cell Tissue Res [Internet]. 2018;372:523–33. http://link.springer.com/https://doi.org/10.1007/s00441-017-2766-x

45. Anjos-Afonso F, Currie E, Palmer HG, Foster KE, Taussig DC, Bonnet D. CD34 – Cells at the Apex of the Human Hematopoietic Stem Cell Hierarchy Have Distinctive Cellular and Molecular Signatures. Cell Stem Cell [Internet]. 2013;13:161–74. https://linkinghub.elsevier.com/retrieve/pii/S193459091300218X

46. Sumide K, Matsuoka Y, Kawamura H, Nakatsuka R, Fujioka T, Asano H et al. A revised road map for the commitment of human cord blood CD34-negative hematopoietic stem cells. Nat Commun [Internet]. 2018;9:2202. http://www.nature.com/articles/s41467-018-04441-z

47. Sonoda Y. Immunophenotype and functional characteristics of human primitive CD34-negative hematopoietic stem cells: the significance of the intra-bone marrow injection. J Autoimmun. 2008. pp. 136–44.

48. Josefsen D, Forfang L, Dyrhaug M, Blystad AK, Stokke T, Smeland EB et al. Side population cells in highly enriched CD34-positive cells from peripheral blood progenitor cells identify an immature subtype of hematopoietic progenitor cells but do not predict time to engraftment in patients treated with high-dose therapy. Eur J Haematol [Internet]. 2011;87:494–502. https://doi.org/10.1111/j.1600-0609.2011.01681.x

49. Pranke P, Hendrikx J, Debnath G, Alespeiti G, Rubinstein P, Nardi N et al. Immunophenotype of hematopoietic stem cells from placental/umbilical cord blood after culture. Brazilian Journal of Medical and Biological Research [Internet]. 2005;38:1775–89. http://www.scielo.br/scielo.php?script=sci_arttext&pid=S0100-879X2005001200006&lng=en&tlng=en

50. Notta F, Doulatov S, Laurenti E, Poeppl A, Jurisica I, Dick JE. Isolation of single human hematopoietic stem cells capable of Long-Term Multilineage Engraftment. Proc Nati Acad Sci USA. 2011;333:1209.

51. Majeti R, Park CY, Weissman IL. Identification of a hierarchy of multipotent hematopoietic progenitors in human cord blood. Cell Stem Cell. 2007;1:635–45.

52. Bari S, Zhong Q, Fan X, Poon Z, Lim AST, Lim TH, et al. Ex vivo expansion of CD34 + CD90 + CD49f + hematopoietic stem and progenitor cells from non-enriched umbilical cord blood with azole compounds. Stem Cells Transl Med. 2018;7:376–93.

53. Zeng R, Liu Y, Jiang Z-J, Huang J-P, Wang Y, Li X-F et al. EPB41L3 is a potential tumor suppressor gene and prognostic indicator in esophageal squamous cell carcinoma. Int J Oncol [Internet]. 2018; http://www.spandidos-publications.com/10.3892/ijo.2018.4316

## Publisher's note